Electronic Supplementary Material (ESI) for Journal of Materials Chemistry A.

Supporting Information

Mutual modulation via charge transfer and unpaired electrons of catalytic site for superior intrinsic activity of N_2 reduction: from high-throughput computations assisted with machine learning perspective

Zheng Shu,[a] Hejin Yan,[a] Hongfei Chen,[a] Yongqing Cai[a]

[a]Joint Key Laboratory of the Ministry of Education, Institute of Applied Physics and Materials Engineering, University of Macau, Taipa, Macau, China

Email: yongqingcai@um.edu.mo

Machine Learning and Feature Importance.

The shallow and deep learning algorithms were implemented using *sklearn*[1] and *keras*[2] in python language. The eligible catalysts are labeled as "1" while ineligible are "0". Cross-validation was adopted for a robust way of evaluating generalization ability. The most commonly used approaches of cross-validation with k-fold cross-validation and 4-fold cross-validation were used for model selection. Decision tree (DT), random forest (RF) and fully connected neural network (FCNN) were used for model evaluation. Permutation importance (PI)[4] method implemented by *eli5* package was utilized to the analysis of feature importance for RF algorithms.

Decision tree (DT) is a simple but widely used model in machine learning[5,6]. It can divide input space into different regions gradually. The most commonly used algorithm is classification and regression tree (CART) which is based on binary tree structure. And the default algorithm of decision tree in scikit-learn is CART. For each node, it creates two subregions according to Gini index, which is defined by:

$$Gini(p) = \sum_{k=1}^{K} p_k(1 - p_k) = 1 - \sum_{k=1}^{K} p_k^2$$

where p_k is the probability of class *k*. *K* is the total number of classes. Next, Gini index will be calculated in the condition of feature A.

$D_1 = \{(x,y) \in D \,|\, A(x) = a\}, D_2 = D - D_1$

$$Gini(D,A) = \frac{|D_1|}{|D|} Gini(D_1) + \frac{|D_2|}{|D|} Gini(D_2)$$

where feature A splits samples set D into subsets D_1 and D_2. For each node, condition Gini condition is calculated and the feature *X* which possesses the maximum value of Gini condition is regarded as the splitting feature. In other words, the splitting feature in the root node is the most important feature for the question. Based on this principle, testing the samples recursively and assigning them to child nodes until samples reach the leaf node. After the process of growing of tree, pruning is used for generalization enhancement. Explicit visualization and explanation easily are the greatest advantages of decision tree. The visualization diagram of decision tree in this work was plotted by *graphviz* 0.16.

Random forest (RF) is an ensemble algorithm based on DT which adopts bagging mechanism[5,6]. It is a more robust algorithm than single DT with a collection of randomized, independent DTs. Each DT makes the prediction independently, then giving the eventual decision according to the principle "Minority is subordinate to majority". Different from DT algorithm, RF is hard to visualize. Instead, feature importance comparison of RF is the common method to measure dominant feature. The feature importance of permutation importance was performed by *eli5* 0.11.0.

Fully connected neural network (FCNN) is a stack of multilayer perception to

learn representations with multiple abstraction level[7]. The FCNN usually consists of input layer, multiple hidden layers and output layer, each of them can be adjusted by backpropagation algorithm. The formula of FCNN can be described by:

$$f(x) = f^{(3)}\left(f^{(2)}\left(f^{(1)}(wx + b)\right) + b\right) + b.....$$

where w is the weights and b is the bias of the network. An objective function which can measure errors between output value and label of training data is computed in the training process. The adjustable parameters called weights and bias are updated by gradient descent algorithm. A non-linear function $f(\cdot)$ is usually followed by the layer to create nonlinear representations, such as rectified linear unit (ReLU) $f(z) = \max(0,z)$. The output layer is activated by sigmoid function to represent probability, which can be formulated:

$$\sigma(x) = \frac{1}{1 + e^{-x}}$$

The FCNN used in this work were constructed by *keras* 2.6.0 while other machine learning algorithms were implemented by *scikit-learn* 0.23.2.

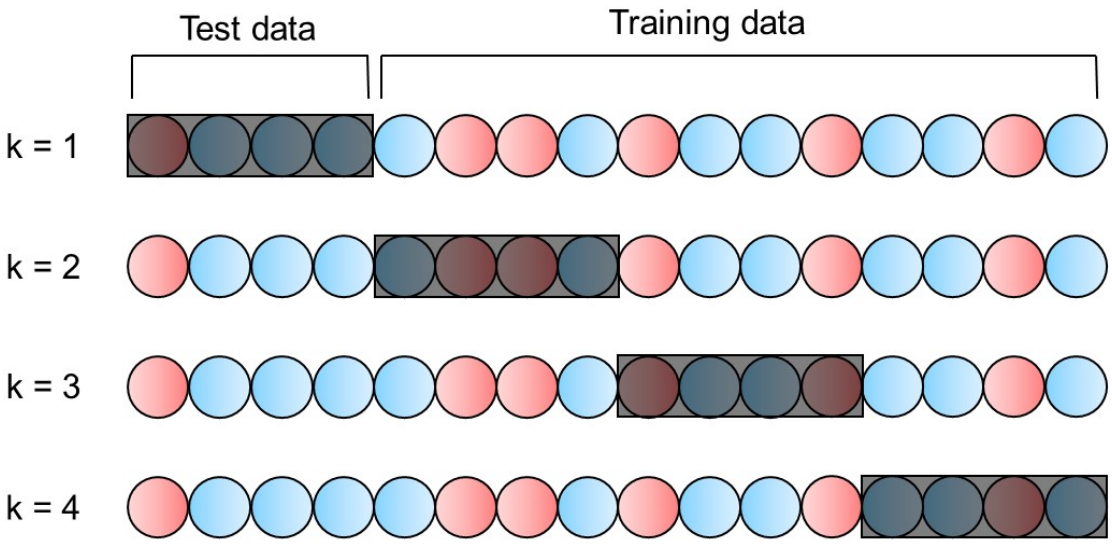

Fig. S1 Sketch map for 4-fold cross-validation. Each fold contains 26 data point before data augmentation. Different colors (blue and red) represent the class 0 or 1.

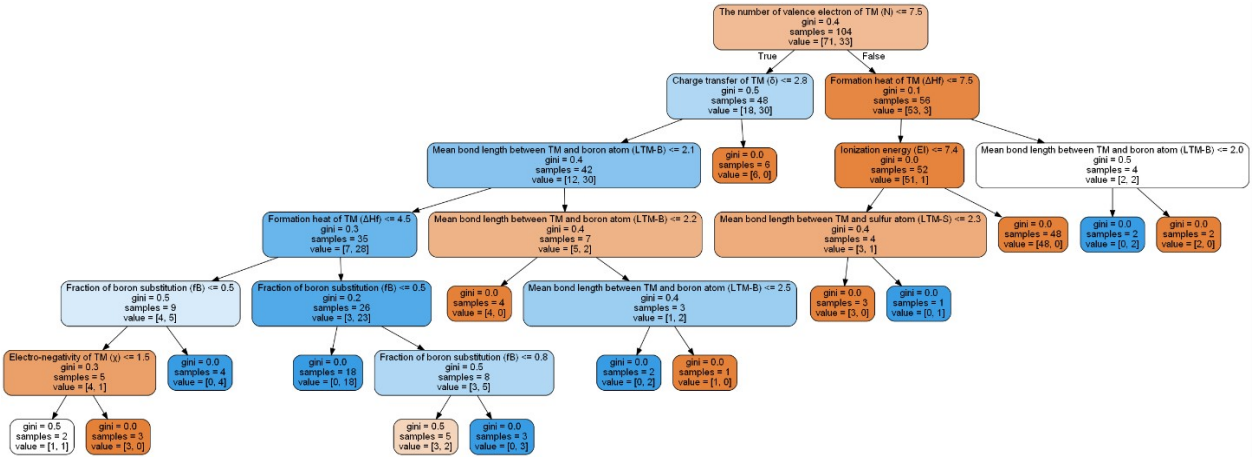

Fig. S2 The decision process of decision Tree (DT). The blue and yellow boxes represent positive and negative samples.

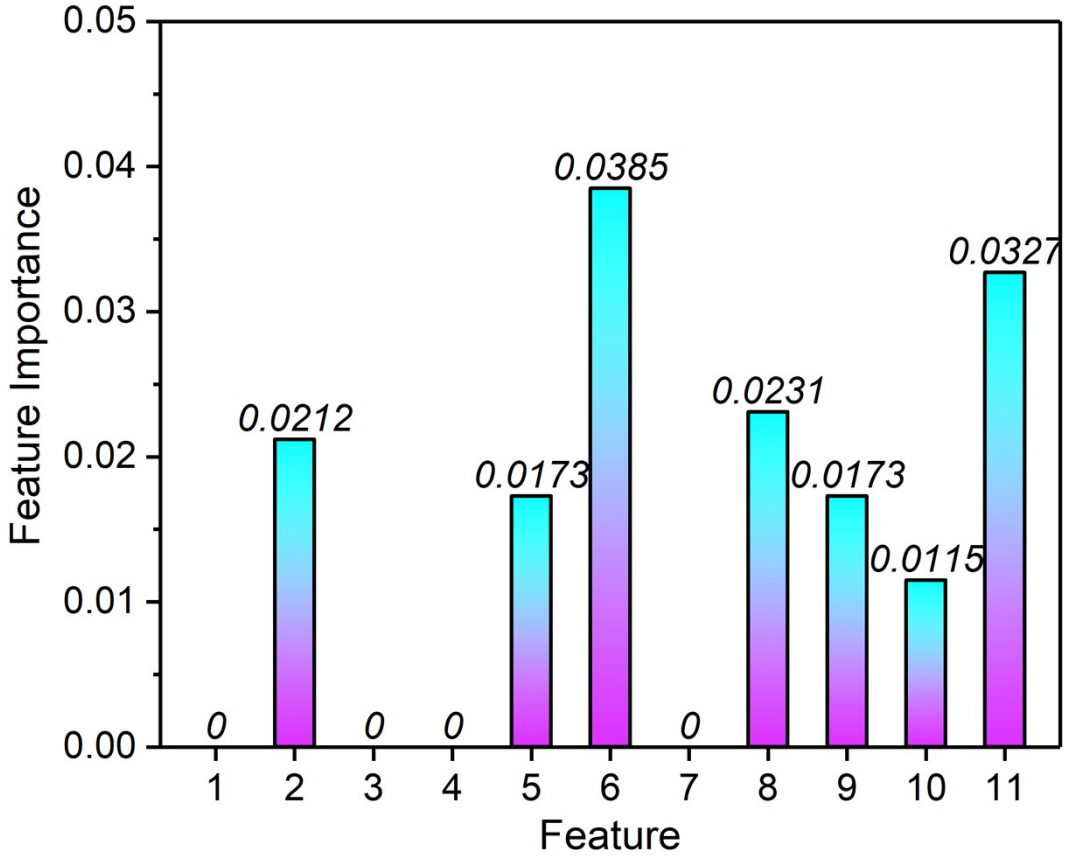

Fig. S3 The ranking of most important features by random forest (RF) using permutation importance (PI) method. Feature 1 to 11 represent Z, ΔH_f, R, χ, E_I, N, $N_{ie\text{-}d}$, δ, $L_{TM\text{-}S}$, $L_{TM\text{-}B}$ and f_B, respectively.

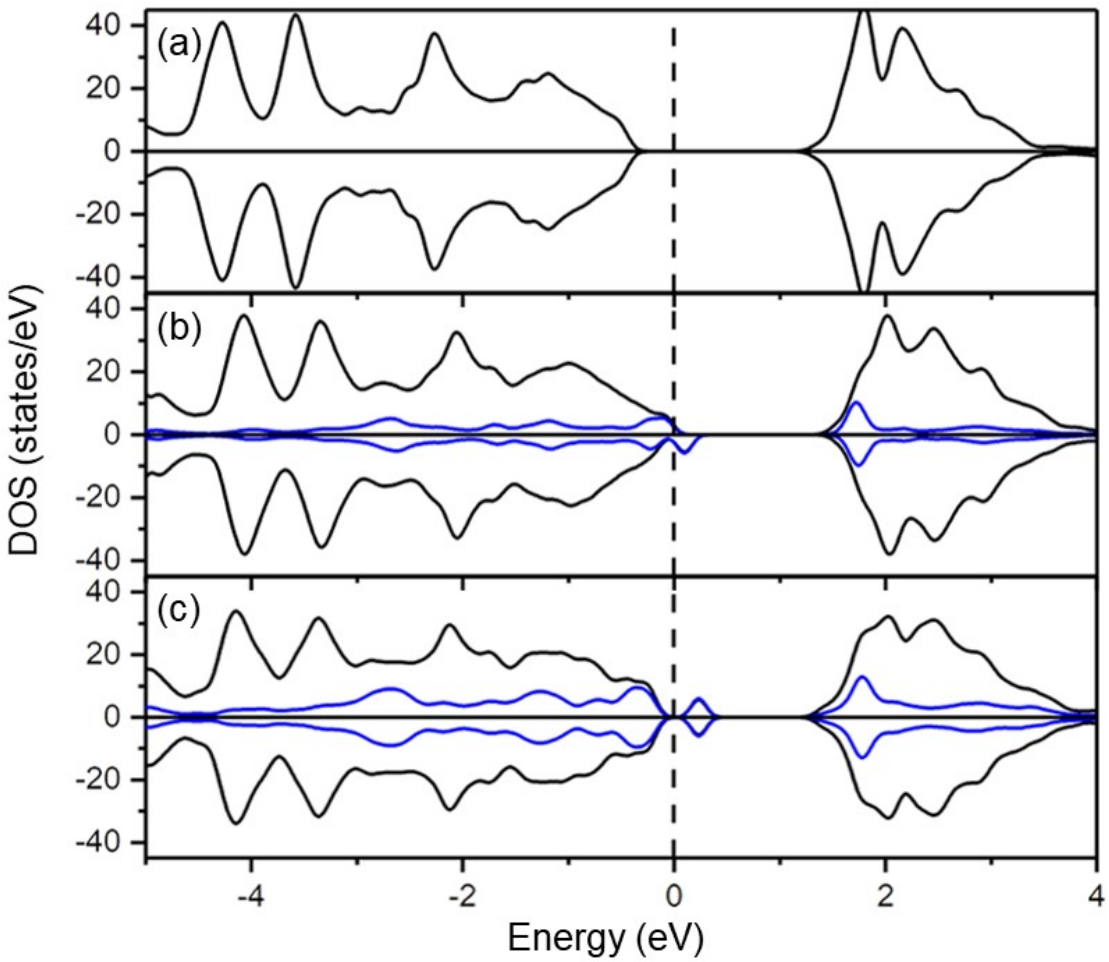

Fig. S4 The DOS of (a) pristine, (b) 1Bs@MoS_2 and (c) 2Bs@MoS_2. The black and blue curves represent total DOS and partial density of states (PDOS) of substitutional boron atom. The Fermi level represented by dashed lines is set to zero.

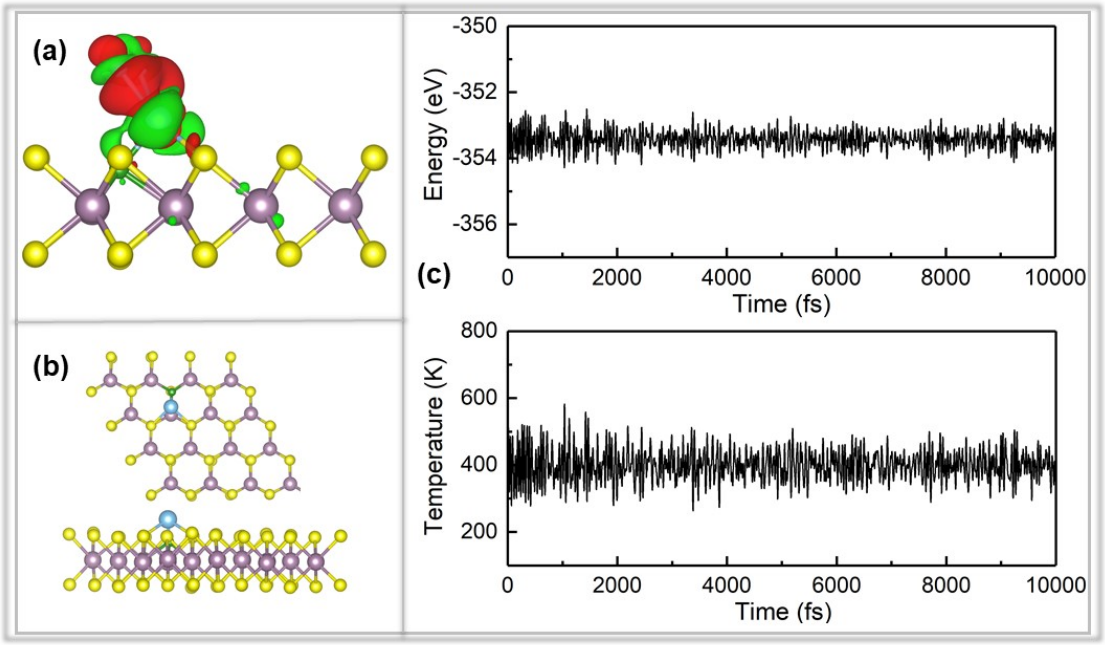

Fig. S5 (a) The differential charge density of 1Bs-Ti@MoS_2 with the adsorbed N_2. The red (green) color represents the positive (negative) of electrons upon adsorption of N_2. (b) The atomic structure after AIMD simulation with 10 ps. (c) Fluctuations of temperature and energy of AIMD simulation at 400 K for 10 ps with a time step of 2 fs.

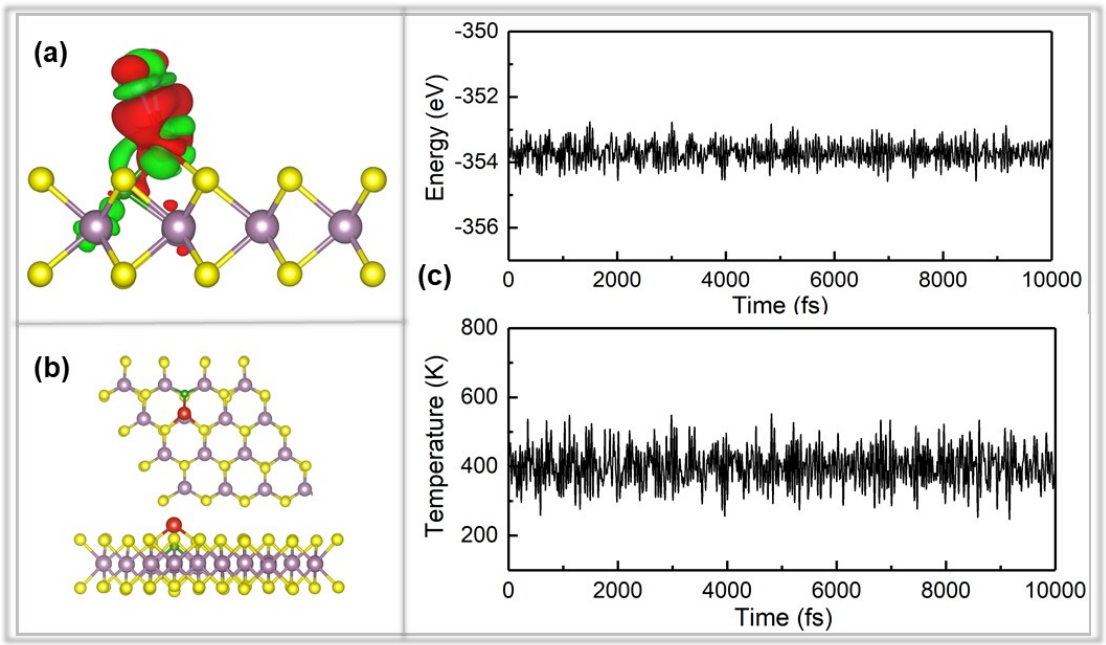

Fig. S6 (a) The differential charge density of 1Bs-V@MoS_2 with the adsorbed N_2. The red (green) color represents the positive (negative) of electrons upon adsorption of N_2. (b) The atomic structure after AIMD simulation with 10 ps. (c) Fluctuations of temperature and energy of AIMD simulation at 400 K for 10 ps with a time step of 2 fs.

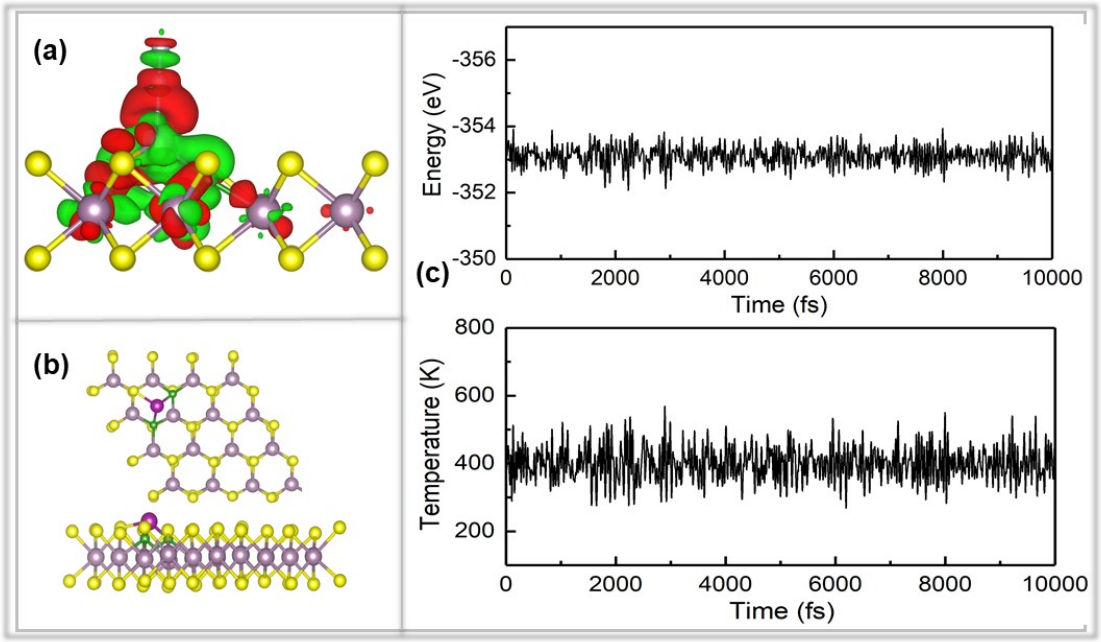

Fig. S7 (a) The differential charge density of 2Bs-Mn@MoS_2 with the adsorbed N_2. The red (green) color represents the positive (negative) of electrons upon adsorption of N_2. (b) The atomic structure after AIMD simulation with 10 ps. (c) Fluctuations of temperature and energy of AIMD simulation at 400 K for 10 ps with a time step of 2 fs.

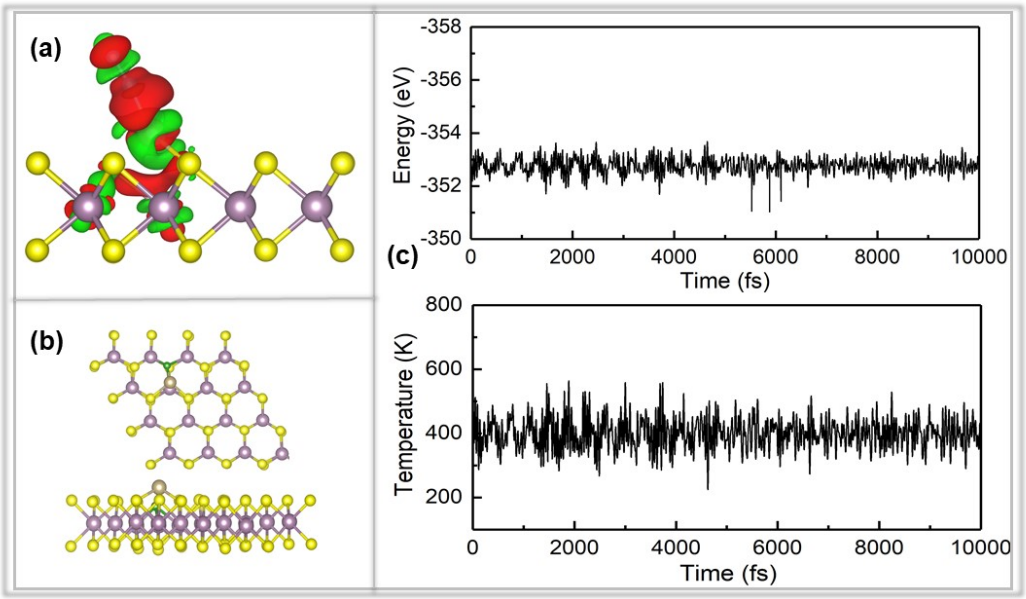

Fig. S8 (a) The differential charge density of 1Bs-Os@MoS_2 with the adsorbed N_2. The red (green) color represents the positive (negative) of electrons upon adsorption of N_2. (b) The atomic structure after AIMD simulation with 10 ps. (c) Fluctuations of temperature and energy of AIMD simulation at 400 K for 10 ps with a time step of 2 fs.

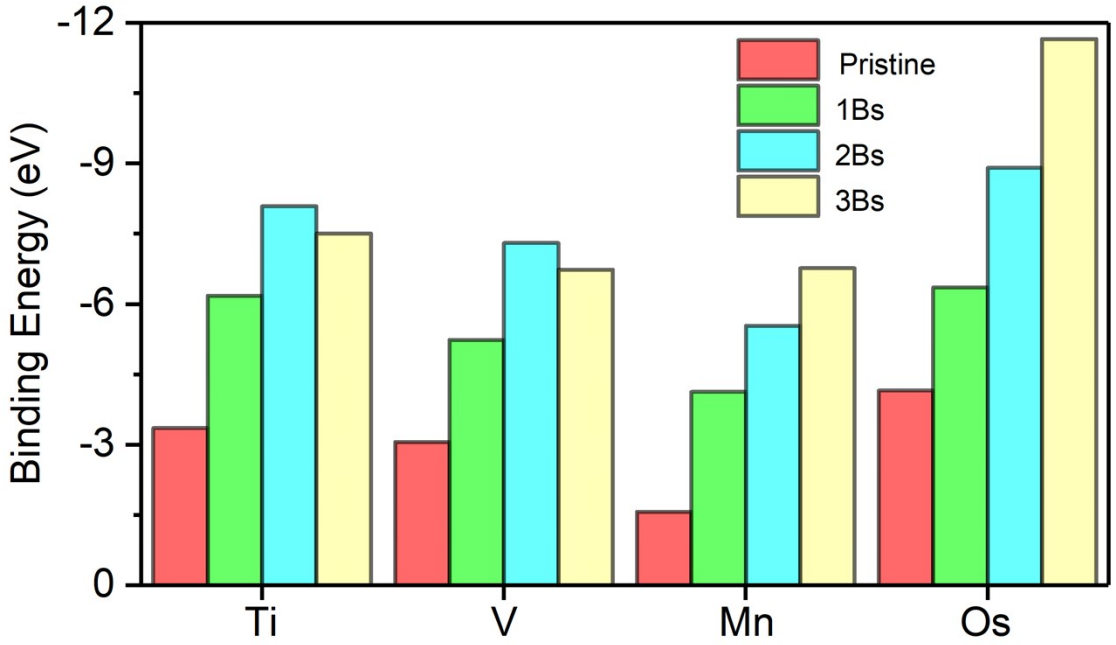

Fig. S9 The binding energies (E_b) of transition metals (Ti, V, Mn and Os) with different fraction of boron doping. $E_b = E_{sub\text{-}TM} - E_{sub} - E_{TM}$, where $E_{sub\text{-}TM}$, E_{sub} and E_{TM} represent the energies of *n*Bs-TM@MoS_2 (*n* = 0, 1, 2, 3), *n*Bs@MoS_2 (*n* = 0, 1, 2, 3) and single-atom TM, respectively.

Tab. S1 Gibbs free energy change of N_2 absorption and first hydrogenation via end-on and side-on pattern for all SAC candidates.

SACs	N_2 absorption (end-on) / eV	First hydrogenation (end-on) / eV	N_2 absorption (side-on) /eV	First hydrogenation (side-on) / eV
Pristine-Sc	-0.99	0.86	-0.94	0.25
Pristine-Ti	-1.22	0.96	-1.06	0.31
Pristine-V	-1.21	1.03	-0.74	0.49
Pristine-Cr	-0.96	0.79	-0.83	0.76
Pristine-Mn	-1.22	0.87	-1.02	0.87
Pristine-Fe	-1.17	0.88	-1.52	1.69
Pristine-Co	-1.30	0.94	-0.73	0.92
Pristine-Ni	-1.02	1.74	-0.53	1.69
Pristine-Cu	-0.50	1.30		
Pristine-Zn				
Pristine-Zr	-1.23	0.71	-1.22	0.15
Pristine-Mo	-1.33	0.44	-1.04	0.27
Pristine-Tc	-1.20	0.39	-0.60	0.43
Pristine-Ru	-1.12	0.69	-0.53	0.70
Pristine-Rh	-1.03	1.08	-0.59	0.90
Pristine-Pd	-0.66	1.76		
Pristine-Ag	-0.22	1.55		
Pristine-Cd				
Pristine-Hf	-1.27	0.59	-1.34	-0.01
Pristine-Ta	-1.69	0.49	-1.54	-0.20
Pristine-W	-1.66	0.25	-1.79	0.18
Pristine-Re	-1.71	0.27	-1.33	0.35
Pristine-Os	-1.60	0.37	-0.87	0.46
Pristine-Ir	-1.44	0.65	-0.78	0.69
Pristine-Pt	-1.07	1.70	-0.53	1.62
Pristine-Au				
$1B_S$-Sc	-0.47	1.52	-0.43	0.87
$1B_S$-Ti	-0.76	0.64	-0.58	0.16
$1B_S$-V	-0.89	0.79	-0.71	0.22
$1B_S$-Cr	-1.69	1.65	-1.53	1.18

$1B_S$-Mn	-0.86	0.95	-0.06	0.48
$1B_S$-Fe	-0.35	0.11	-1.25	1.51
$1B_S$-Co	-1.19	0.87	-0.67	0.76
$1B_S$-Ni	-2.09	2.12	-1.79	2.35
$1B_S$-Cu	-4.21	3.41		
$1B_S$-Zn	0.06	1.13		
$1B_S$-Zr	-1.11	0.67	-0.95	0.46
$1B_S$-Mo	-1.04	0.45	-1.15	0.31
$1B_S$-Tc	-0.98	0.45	-0.61	0.44
$1B_S$-Ru	-1.00	0.61	-0.62	0.51
$1B_S$-Rh	-0.91	0.97	-0.63	1.00
$1B_S$-Pd	-0.64	1.12	-0.31	1.52
$1B_S$-Ag	-0.35	1.85		
$1B_S$-Cd				
$1B_S$-Hf	-0.79	0.74	-0.72	-0.28
$1B_S$-Ta	-1.31	0.55	-1.42	0.04
$1B_S$-W	-1.52	0.40	-1.67	0.02
$1B_S$-Re	-1.54	0.24	-1.39	0.32
$1B_S$-Os	-1.50	0.25	-1.19	0.28
$1B_S$-Ir	-1.42	0.7	-1.04	0.77
$1B_S$-Pt	-1.12	1.07	-0.56	1.15
$1B_S$-Au	-0.31	1.50		
$2B_S$-Sc	-0.42	-0.53		
$2B_S$-Ti	-0.24	-0.23		
$2B_S$-V	-0.53	0.92	-0.91	0.89
$2B_S$-Cr	-0.43	0.44	-0.84	0.83
$2B_S$-Mn	-0.26	0.39	-0.26	0.4
$2B_S$-Fe	-1.12	0.58	-1.01	0.73
$2B_S$-Co	-1.75	0.83	-1.15	0.98
$2B_S$-Ni	-1.69	1.31	-1.16	1.22
$2B_S$-Cu	-0.37	1.46		
$2B_S$-Zn	-0.14	1.52		
$2B_S$-Zr	-0.20	1.46		
$2B_S$-Mo	-0.64	1.08		
$2B_S$-Tc	-0.47	0.76	-0.17	0.43
$2B_S$-Ru	-0.94	1.07	-0.54	0.94

$2B_S$-Rh	-1.04	0.99	-0.71	0.99
$2B_S$-Pd	-0.30	1.30		
$2B_S$-Ag	-0.21	1.67		
$2B_S$-Cd				
$2B_S$-Hf	-0.21	1.28	0.10	0.38
$2B_S$-Ta	-0.71	1.06	-0.25	0.15
$2B_S$-W	-0.94	0.81	-0.34	0.08
$2B_S$-Re	-1.12	0.73	-0.64	0.2
$2B_S$-Os	-0.83	-0.51		
$2B_S$-Ir	-1.53	0.65		
$2B_S$-Pt	-0.37	0.98		
$2B_S$-Au	-0.25	1.48		
$3B_S$-Sc	-1.11	2.22		
$3B_S$-Ti	-2.73	1.08	-2.46	0.37
$3B_S$-V	-0.98	1.32	-0.83	0.44
$3B_S$-Cr	-0.01	-0.49	-0.13	0.05
$3B_S$-Mn	-0.69	-0.07	-1.09	0.59
$3B_S$-Fe	-0.60	0.86	-0.98	1.76
$3B_S$-Co	-0.86	1.01	-0.56	1.41
$3B_S$-Ni	-0.67	1.27	-0.38	-0.45
$3B_S$-Cu	-0.56	1.46	-0.64	1.83
$3B_S$-Zn	-0.77	1.70		
$3B_S$-Zr	-0.42	-0.08	-0.11	-0.39
$3B_S$-Mo	-0.10	0.07	0.34	-0.83
$3B_S$-Tc	0.20	-0.21	-0.11	0.21
$3B_S$-Ru	-0.46	0.91	-0.55	1.02
$3B_S$-Rh	-0.48	1.57	-0.24	1.37
$3B_S$-Pd	-0.37	1.72	-0.01	1.63
$3B_S$-Ag	-0.20	1.90		
$3B_S$-Cd	0.68	3.52		
$3B_S$-Hf	-2.00	0.49		
$3B_S$-Ta	-1.08	1.08	0.31	-0.96
$3B_S$-W	-0.42	0.72	0.23	-1.44
$3B_S$-Re	-0.61	0.57	-0.01	-0.08
$3B_S$-Os	-0.64	1.10	0.01	0.70
$3B_S$-Ir	-0.58	1.22	-0.20	1.07

$3B_S$-Pt	-0.57	1.31	-0.14	1.26
$3B_S$-Au	-0.25	1.64		

Tab. S2 ΔG_{H^*} for SAC candidates. Only those candidates whose energy injection of N_2 adsorption and first hydrogenation meet criterions were considered.

	Pristine MoS_2	$1B_S$@ MoS_2	$2B_S$@ MoS_2	$3B_S$@ MoS_2
Sc	-0.78		2.12	
Ti	-0.51	-0.01	1.99	2.77
V	-0.38	0.06		3.98
Cr			0.25	2.16
Mn		-0.87	0.21	0.65
Fe		-0.75		
Co				
Ni				-2.16
Cu				
Zn				
Zr	-0.88	-0.38		1.73
Mo	-0.67	-0.11		1.25
Tc	-0.66	-0.34	-0.16	0.95
Ru		-0.22		
Rh				
Pd				
Ag				
Cd				
Hf	-0.66	0.40		-2.15
Ta	-0.93	-0.99	-0.31	
W	-1.09	-1.03	-0.51	
Re	-1.27	-1.02	-1.00	0.42
Os	-0.76	-0.90	-1.91	
Ir				
Pt				
Au				

Tab. S3 Vibrational frequencies of intermediate species and zero-point energy (E_{ZPE}) with entropy correction (-*TS*) at standard condition. The $2B_S$-Mn@MoS_2 is used as representative data and calculations are listed.

Species	Vibrational Frequencies (cm^{-1})						E_{ZPE} (eV)	-*TS* (eV)	E_{ZPE}-*TS* (eV)
*N-*N	1925.60	477.47	300.48	156.93	116.28	67.08	0.18	-0.15	0.03
*N-*NH	3190.26	1646.85	1103.51	775.27	550.74	391.42	0.50	-0.13	0.37
	184.08	133.37	106.39						
*NH-*NH	3330.03	3276.67	1309.11	1264.51	1052.83	735.12	0.76	-0.14	0.62
	550.67	409.59	299.89	121.65	82.04	53.89			
NH-NH_2	3499.07	3393.55	3385.08	1595.10	1311.78	1110.79	1.15	-0.16	0.99
	1063.70	825.51	688.33	625.30	465.38	353.61			
	161.75	109.92	95.55						
NH_2-NH_2	3529.25	3490.24	3414.31	3409.93	1526.42	1513.00	1.42	-0.16	1.26
	892.23	784.97	721.37	694.65	650.62	597.28			
	513.06	370.43	336.63	218.81	169.78	121.45			
NH_2-NH_3	3509.22	3494.59	3450.22	3389.30	3322.11	1609.26	1.72	-0.22	1.50
	1596.46	1545.41	1184.63	790.22	646.68	617.69			
	599.17	555.92	375.09	326.66	292.75	186.20			
	154.35	131.54	99.64						
*NH_3	3478.17	3420.00	3254.69	1597.72	1577.51	1208.59	1.03	-0.13	0.90
	644.98	624.12	394.30	194.43	160.09	92.06			
*N-N	2270.13	329.30	239.71	227.29	40.96	32.76	0.19	-0.20	-0.01
*N-NH	3200.68	1753.93	1081.76	517.03	455.70	350.48	0.48	-0.15	0.33
	282.80	83.93	68.64						
*N-NH_2	3492.98	3361.94	1585.55	1448.90	1182.63	540.53	0.81	-0.11	0.70
	403.90	356.73	344.44	241.21	113.97	23.99			
*N	1017.32	167.20	112.56				0.08	-0.07	0.01
*NH	3463.66	885.12	544.88	418.33	157.65	150.20	0.34	-0.08	0.26
*NH_2	3538.52	3433.71	1454.59	633.69	545.38	515.54	0.66	-0.11	0.55
	299.05	144.54	135.73						
*NH-NH	3236.30	3154.77	1499.64	1401.39	1272.85	995.51	0.80	-0.13	0.67
	514.30	413.44	228.68	203.50	64.54	57.13			
*NH-NH_2	3554.17	3419.63	3367.95	1591.32	1436.63	1248.24	1.14	-0.19	0.95
	1161.71	676.66	515.30	502.34	362.61	260.47			

	196.47	114.96	42.53						
*NH_2-NH_2	3440.60	3406.93	3347.30	3268.95	1627.20	1572.27	1.48	-0.27	1.21
	1420.49	1187.64	1099.94	1056.89	897.97	599.03			
	447.49	256.87	163.54	145.32	39.46	13.84			
H_2							0.27	-0.42	-0.15
N_2							0.16	-0.60	-0.44
NH_3							0.94	-0.60	0.34

Tab. S4 The ΔG_{max} of all eligible catalysts and corresponding reaction process.

Catalysts	ΔG_{max} (eV)	Reaction process	Pathway
$Sc@MoS_2$	0.93	*NH-*NH_2 → *NH_2-*NH_2	enzymatic
$Ti@MoS_2$	0.86	*NH-*NH_2 → *NH_2-*NH_2	enzymatic
$V@MoS_2$	0.66	*NH-*NH_2 → *NH_2-*NH_2	enzymatic
$Zr@MoS_2$	0.97	*NH-*NH_2 → *NH_2-*NH_2	enzymatic
$Mo@MoS_2$	0.44	*N-N → *N-NH	distal
$Tc@MoS_2$	0.43	*N-N → *N-NH	distal
$Hf@MoS_2$	1.25	*NH-*NH_2 → *NH_2-*NH_2	enzymatic
$Ta@MoS_2$	1.22	*NH-*NH_2 → *NH_2-*NH_2	enzymatic
$W@MoS_2$	0.5	*NH_2 → *NH_3	enzymatic
$Re@MoS_2$	0.4	*NH_2 → *NH_3	enzymatic
$Os@MoS_2$	0.37	*N-N → *N-NH	distal
1Bs-$Ti@MoS_2$	0.37	*NH-*NH_2 → *NH_2-*NH_2	enzymatic
1Bs-$V@MoS_2$	0.33	*NH-*NH_2 → *NH_2-*NH_2	enzymatic
1Bs-$Zr@MoS_2$	0.64	*NH_2 → *NH_3	enzymatic
1Bs-$Mo@MoS_2$	0.45	*N-N → *N-NH	distal
1Bs-$Tc@MoS_2$	0.45	*N-N → *N-NH	distal
1Bs-$Ru@MoS_2$	0.51	*N-*N → *N-*NH	enzymatic
1Bs-$Hf@MoS_2$	0.71	*NH-*NH_2 →	enzymatic

		$*NH_2$-$*NH_2$	
1Bs-Ta@MoS_2	1.34	$*NH$-$*NH_2$ → $*NH_2$-$*NH_2$	enzymatic
1Bs-W@MoS_2	0.50	*N-N → *N-NH	distal
1Bs-Re@MoS_2	0.45	*N-N → *N-NH	distal
1Bs-Os@MoS_2	0.25	*N-N → *N-NH	distal
2Bs-Sc@MoS_2	1.28	$*NH_2$ → $*NH_3$	distal
2Bs-Ti@MoS_2	0.82	$*NH_2$ → $*NH_3$	distal
2Bs-Cr@MoS_2	0.44	*N-N → *N-NH	distal
2Bs-Mn@MoS_2	0.39	*N-N → *N-NH	distal
2Bs-Tc@MoS_2	0.43	*N-*N → *N-*NH	enzymatic

References

1. F. Pedregosa, G. Varoquaux, A. Gramfort, V. Michel, B. Thirion, O. Grisel, M. Blondel, P. Prettenhofer, R. Weiss, V. Dubourg, J. Vanderplas, A. Passos, D. Cournapeau, M. Brucher, M. Perrot and É. Duchesnay, *J. Mach. Learn. Res.*, 2011, **12**, 2825–2830.

2. C. Francois, *Deep learning with Python*, Manning Publications Company, 2017.

3. R. Forests, *Machine Learning*, 2001, **45**, 5–32.

4. C. M. Bishop, *Pattern recognition and machine learning*, Springer, 2006.

5. M. M. Gaber, *Scientific Data Mining and Knowledge Discovery: Principles and Foundations*, Springer, 2009.

6. Y. LeCun, Y. Bengio and G. Hinton, *Nature*, 2015, **521**, 436-444.